Int J Softw Tools Technol Transfer
DOI 10.1007/s10009-017-0458-1

REGULAR PAPER

Hybrid automata: from verification to implementation

Stanley Bak[1] · Omar Ali Beg[2] · Sergiy Bogomolov[3] · Taylor T. Johnson[4] · Luan Viet Nguyen[2] · Christian Schilling[5]

Abstract Hybrid automata are an important formalism for modeling dynamical systems exhibiting mixed discrete–continuous behavior such as control systems and are amenable to formal verification. However, hybrid automata lack expressiveness compared to integrated model-based design frameworks such as the MathWorks' Simulink/ Stateflow (SLSF). In this paper, we propose a technique for correct-by-construction compositional design of cyber-physical systems (CPS) by embedding hybrid automata into SLSF models. Hybrid automata are first verified using verification tools such as SpaceEx and then automatically translated to embed the hybrid automata into SLSF models such that the properties verified are transferred and maintained in the translated SLSF model. The resultant SLSF model can then be used for automatic code generation and deployment to hardware, resulting in an implementation. The approach is implemented in a software tool building on the HyST model transformation tool for hybrid systems. We show the effectiveness of our approach on a CPS case study—a closed-loop buck converter—and validate the overall correct-by-construction methodology: from formal verification to implementation in hardware controlling an actual physical plant.

DISTRIBUTION A. Approved for public release; Distribution unlimited. (Approval AFRL PA #88ABW-2015-2402).

✉ Christian Schilling
schillic@informatik.uni-freiburg.de

[1] Air Force Research Laboratory, Dayton, OH, USA

[2] University of Texas at Arlington, Arlington, TX, USA

[3] Australian National University, Canberra, Australia

[4] Vanderbilt University, Nashville, TN, USA

[5] University of Freiburg, Freiburg im Breisgau, Germany

Keywords Hybrid automata · Model-based design · Simulink/Stateflow

1 Introduction

In this paper, we present the theory and associated implementation for the translation of hybrid automaton models (used for verification) to the MathWorks Simulink/Stateflow (SLSF) models, subsequently used for design refinement, simulation, implementation, and code generation for target embedded hardware. Our approach is particularly useful if the design process is structured in a bottom-up fashion. In other words, we assume that the individual system components are first modeled in detail, such as modeling a control algorithm as a hybrid automaton and verifying properties (typically safety) for it. These components are then linked together to form the whole system under consideration within SLSF. This leads to overall system models consisting of heterogeneous components where a number of components are modeled as hybrid automata, but the entire system may be too complex to formally model and verify. In the last decade, a number of powerful formal design, analysis, and verification tools for hybrid automata such as SpaceEx [8–11,21] and Flow* [16] have emerged. In our proposed approach, a designer can ensure the correctness of individual components before using our translation process to link the system together in SLSF (see Fig. 1).

We introduce a technique to automatically convert the hybrid automata into *trajectory-equivalent* SLSF diagrams. By trajectory-equivalent, we mean that behaviors (trajectories) of the translated SLSF diagram match those of the original hybrid automaton. One technical challenge is that hybrid automata and SLSF differ in semantics: A hybrid automaton is typically defined with *may*-semantics with

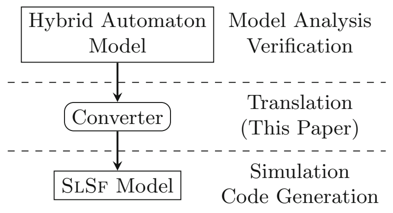

Fig. 1 High-level overview of the model-based design process enabled by this work. Verification using the hybrid automaton is first performed in a hybrid systems model checker, and then, we automatically generate a trajectory-equivalent SLSF diagram. The diagram can then be embedded into a more complex system, possibly with other, unverified components (because they are too large to verify, exist for legacy reasons, etc.), and can then be used for code generation and implementation in actual systems

respect to the discrete transitions, whereas SLSF employs *must*-semantics. In other words, a transition in SLSF is taken as soon as the transition guard is enabled subject to some numerical aspects with zero-crossing detection, whereas the hybrid automaton still has the freedom to stay in the current location as long as the location invariant has not been violated. In case of nondeterministic hybrid automata, trajectory equivalence means that the behaviors of the original hybrid automaton will be exhaustively explored. Our approach incorporates additional randomization steps into the resulting SLSF diagram. In this way, in every run, the diagram produces a possibly different trace that still reflects a trajectory from the original hybrid automaton semantics. After running more and more simulations, we get a better and better approximation of the reachable state space of the original hybrid automaton.

Related work Significant research has been performed on the translation of SLSF diagrams into other analysis tools, such as hybrid systems model checkers [1,3,7,13,14,29–31,36,37,40,43]. Agrawal et al. [1] suggest an algorithm to translate SLSF diagrams into the equivalent Hybrid Systems Interchange Format (HSIF) [13,14,36,37] models. The Compositional Interchange Format (CIF) provides a common input language focused on model compositionality for networks of hybrid automata [2]. Alur et al. translated SLSF to linear hybrid automata for applying symbolic analysis to improve test coverage of SLSF [3]. In a different setting, Schrammel et al. [40] consider the translation problem for complex SLSF diagrams where involved treatment of zero-crossings is needed. Manamcheri et al. [29] have developed the tool HyLink to translate a restricted class of SLSF to hybrid automata. Minopoli et al. [30,31] have developed a theory of urgent semantics for hybrid automata and the SL2SX tool that translates a restricted subset of SLSF diagrams to hybrid automata. The application of the above techniques is restricted by the fact that no complete semantics of SLSF is provided (in spite of recent progress [7,12,22,23,29,38]).

In contrast to all these existing works, we consider the converse direction, i.e., to translate a given hybrid automaton into an SLSF diagram. Sanfelice et al. [39] have developed the hybrid equations toolbox (HyEQ) to approximately simulate the hybrid systems that may include Zeno, zero-crossing, and nondeterministic behaviors. However, the applicability of the Simulink Design Verifier (SDV) model checker [42] integrated with SLSF does not apply to this class of models, so verification is not possible. In our setting, we benefit from clear and unambiguous hybrid automata semantics and may formally verify properties of the hybrid automata prior to translating them to SLSF diagrams. Pajic et al. [25,33–35] consider a similar problem of converting timed automata encoded in UPPAAL [27] to SLSF diagrams. However, in their translation, they consider only runs of UPPAAL models that obey the *must*-semantics. In our work, beyond considering the much more expressive framework of hybrid automata (as timed automata are a subclass of hybrid automata), we provide a translation handling the nondeterminism by producing trajectory-equivalent SLSF diagrams. Operational semantics of (purely discrete) SLSF have been developed [23], and alternative formalizations of discrete semantics have been investigated using, for example, translation from SLSF to C [38]. In contrast to these prior works, we focus on continuous-time SLSF diagrams. Another recent line of research focuses on the translation from Hybrid Communicating Sequential Processes (HCSP) to Simulink block diagrams [15,44,45]. In our work, we consider the translation of the hybrid automaton model, which is extensively used in the industry for CPS modeling.

Contributions This paper has four primary contributions. *(a)* This is the first work, as far as we are aware, to provide a translation scheme from hybrid automata to SLSF diagrams, which is useful as part of a model-based design (MBD) process. *(b)* In order to overcome the difference in semantics between the modeling frameworks, we introduce the notion of trajectory equivalence and show how the conversion preserves trajectory equivalence with respect to several sources of nondeterminism in hybrid automata. *(c)* We provide an implementation of the trajectory-equivalent translation scheme as a part of the HyST model translation framework [5], which enables completely automatic translation of existing hybrid automaton models. *(d)* We show the applicability of our contributions in several case studies where hybrid automata are automatically translated to SLSF for simulation, use in larger SLSF diagrams, and deployment to actual hardware. For one case study—a closed-loop buck converter—the entire correct-by-construction MBD process is illustrated, from verification through implementation in hardware. This includes formal verification of the hybrid automaton in SpaceEx, translation to SLSF, code generation for the controller in SLSF, then subsequent compilation, and finally execution in embedded hardware controlling the physical plant.

Paper organization The remainder of the paper is organized as follows: After introducing the necessary background in Sect. 2, we present our trajectory-equivalent translation scheme in Sect. 3. In Sect. 4, we evaluate our approach on four case studies. We conclude in Sect. 5.

2 Preliminaries

In this section, we introduce the preliminaries that are needed for this work. We first define a hybrid automaton model and discuss its semantics and then do the same for SLSF diagrams.

2.1 Hybrid automata

A hybrid automaton is formally defined as follows.

Definition 1 (*Hybrid automaton*) A *hybrid automaton* is a tuple $\mathcal{H} \triangleq (Loc, Var, Init, Flow, Trans, Inv)$ with: *(a)* the finite set of locations Loc, *(b)* the set of continuous variables $Var \triangleq \{x_1, \ldots, x_n\}$ from $\mathbb{R}^n$, *(c)* the initial condition, given by $Init(\ell) \subseteq \mathbb{R}^n$ for each location ℓ, *(d)* the flow, a deterministic function $Flow(\ell)$ from the variables to their derivatives for each location ℓ, *(e)* the discrete transition relation $Trans$, where every transition is a tuple $(\ell, g, \upsilon, \ell')$ with: *(i)* the source location ℓ and the target location ℓ', *(ii)* the guard, given by a constraint g, *(iii)* the update, given by a mapping υ that modifies the variable valuation, and *(f)* the invariant $Inv(\ell) \subseteq \mathbb{R}^n$ for each location ℓ.

We use the common . (dot) notation to specifically indicate components of $\mathcal{H}$ as necessary, e.g., $\mathcal{H}.Var$ are the variables of $\mathcal{H}$.

The semantics of a hybrid automaton $\mathcal{H}$ is defined in terms of trajectories as follows: A *state* of $\mathcal{H}$ is a pair $(\ell, \mathbf{x})$ that consists of a location $\ell \in Loc$ and a point $\mathbf{x} \in \mathbb{R}^n$. Formally, $\mathbf{x}$ is a valuation of the continuous variables in Var. For the following definitions, let $T = [0, \Delta]$ be an interval for some $\Delta \geq 0$.

Definition 2 A *trajectory* of $\mathcal{H}$ from state $s = (\ell, \mathbf{x})$ to state $s' = (\ell', \mathbf{x}')$ is a pair $\rho \triangleq (L, \mathbf{X})$, where $L : T \to Loc$ and $\mathbf{X} : T \to \mathbb{R}^n$ are functions that define for each time point in T the location and the values of the continuous variables, respectively. A sequence of time points where location switches happen in ρ is denoted by $(\xi_i)_{i=0\ldots k} \in T^{k+1}$. In this case, we define the *length* of ρ as $|\xi| = k$. Trajectories $\rho = (L, \mathbf{X})$, and the corresponding sequence $(\xi_i)_{i=0\ldots k}$, must satisfy the following conditions:

(a) $\xi_0 = 0, \xi_i < \xi_{i+1}$, and $\xi_k = \Delta$—the sequence of switching points increases, starts with 0 and ends with Δ,
(b) $L(0) = \ell$, $\mathbf{X}(0) = \mathbf{x}$, $L(\Delta) = \ell'$, $\mathbf{X}(\Delta) = \mathbf{x}'$—the trajectory starts in $s = (\ell, \mathbf{x})$ and ends in $s' = (\ell', \mathbf{x}')$,
(c) $\forall i\ \forall t \in [\xi_i, \xi_{i+1}) : L(t) = L(\xi_i)$—the location is not changed during the continuous evolution,
(d) $\forall i\ \forall t \in [\xi_i, \xi_{i+1}) :\ (\mathbf{X}(t), \dot{\mathbf{X}}(t)) \in Flow(L(\xi_i))$ holds and thus the continuous evolution is consistent with the differential equations of the corresponding location,
(e) $\forall i\ \forall t \in [\xi_i, \xi_{i+1}) : \mathbf{X}(t) \in Inv(L(\xi_i))$—the continuous evolution is consistent with the corresponding invariants, and
(f) $\forall i < k\ \exists (L(\xi_i), g, \upsilon, L(\xi_{i+1})) \in Trans : \mathbf{X}_{end}(i) \in g \wedge \mathbf{X}(\xi_{i+1}) = \upsilon(\mathbf{X}_{end}(i)) \wedge \mathbf{X}_{end}(i) = \lim_{\xi \to \xi_{i+1}^-} \mathbf{X}(\xi)$—every continuous transition is followed by a discrete one, where $\mathbf{X}_{end}(i)$ defines the values of continuous variables immediately before the discrete transition at the time moment ξ_{i+1}.

A state s' is *reachable* from state s if there exists a trajectory from s to s'.

A *symbolic state* $s \triangleq (\ell, \mathcal{R})$ is a pair, where $\ell \in Loc$ and $\mathcal{R}$ is a convex and bounded set consisting of points $\mathbf{x} \in \mathbb{R}^n$. The continuous part $\mathcal{R}$ of a symbolic state is also called *region*. The symbolic state space of $\mathcal{H}$ is called the *region space*. The initial set of states $\mathcal{S}_{init}$ of $\mathcal{H}$ is defined as $\bigcup_\ell (\ell, Init(\ell))$. The reachable state space Reach$(\mathcal{H})$ of $\mathcal{H}$ is defined as the set of symbolic states that are reachable from some initial state in $\mathcal{S}_{init}$, where the definition of reachability is extended accordingly for symbolic states. We refer to the set of all the trajectories of $\mathcal{H}$ starting in $\mathcal{S}_{init}$ by Traj$(\mathcal{H})$. A *safety specification P* is a given set of symbolic states. A hybrid automaton $\mathcal{H}$ *satisfies* a safety specification P iff Reach$(\mathcal{H}) \subseteq P$. We are interested in ensuring that the hybrid automaton is correct, i.e., satisfies P, and then subsequently translate it for simulation, integration, and implementation in SLSF as discussed in the next sections.

2.2 Continuous-time Stateflow diagrams

Simulink is a graphical modeling language for control systems, plants, and software. Stateflow is a state-based graphical modeling language integrated within Simulink. Continuous-time Stateflow diagrams provide methods for modeling hybrid systems that consist of continuous and discrete states and behaviors. In this section, we describe a *restricted subclass of continuous-time Stateflow diagrams* to which we translate a hybrid automaton. In particular, we focus only on continuous-time Stateflow state transition diagrams, and we do not consider models with hierarchical states.

Roughly, a Stateflow state transition diagram may be thought of as an extended state machine with variables of various types. In addition to states, Stateflow diagrams may

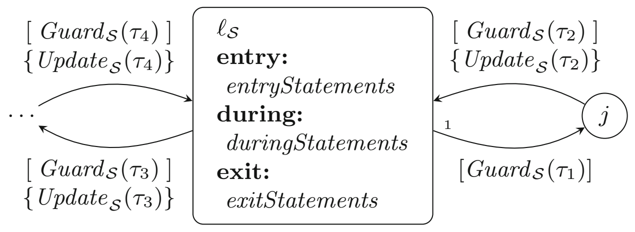

$[\,Guard_{\mathcal{S}}(\tau_4)\,]$
$\{Update_{\mathcal{S}}(\tau_4)\}$
$\ell_{\mathcal{S}}$
entry:
entryStatements
during:
duringStatements
exit:
exitStatements
$[\,Guard_{\mathcal{S}}(\tau_2)\,]$
$\{Update_{\mathcal{S}}(\tau_2)\}$
j
1
$[Guard_{\mathcal{S}}(\tau_1)]$
$[\,Guard_{\mathcal{S}}(\tau_3)\,]$
$\{Update_{\mathcal{S}}(\tau_3)\}$

Fig. 2 Snippet of a general continuous-time Stateflow diagram with a state $\ell_{\mathcal{S}}$, a junction j, and four transitions $\tau_1 - \tau_4$

have junctions that are instantaneous. A transition between states may occur at each simulation time step, whereas multiple junction transitions may occur in a single simulation time step.

A continuous-time Stateflow diagram (see Fig. 2) is roughly analogous to a hybrid automaton, but their behavior differs in several ways. In particular, Stateflow diagrams (1) are deterministic, (2) have urgent transitions with priorities, and (3) have events such as enabled transitions that are determined at runtime by zero-crossing detection algorithms.

We define Stateflow diagrams more formally now.

Definition 3 (*Stateflow diagram*) The tuple $\mathcal{S} \triangleq (Loc_{\mathcal{S}}, Junc_{\mathcal{S}}, Var_{\mathcal{S}}, Trans_{\mathcal{S}}, Actions_{\mathcal{S}})$ defines the *Stateflow diagram*. Here, *(a)* $Loc_{\mathcal{S}}$ is a finite set of *states* (also known as *locations*), *(b)* the junctions $Junc_{\mathcal{S}}$ are like locations, but all of which may be evaluated in a single simulation event step (i.e., they are instantaneous "states"), *(c)* $Var_{\mathcal{S}}$ is a finite set of variables of various types, and for our formalization we assume that they are real-valued, *(d)* the $Actions_{\mathcal{S}}(\ell_{\mathcal{S}})$ for each location $\ell_{\mathcal{S}}$ are actions described by MATLAB or C statements that are performed at different event times subdivided into `entry`, `during`, and `exit` actions, where the `entry` (resp. `exit`) action is executed only once when entering (resp. exiting) the state and the `during` action performs the continuous-time evolution of the variables of $Var_{\mathcal{S}}$ according to a differential equation (this happens strictly between entering and exiting), *(e)* the discrete transition relation $Trans_{\mathcal{S}}$ where every transition $\tau \in Trans_{\mathcal{S}}$ is formally defined as a tuple $(\ell_{\mathcal{S}}, Guard_{\mathcal{S}}, Update_{\mathcal{S}}, TP_{\mathcal{S}}, \ell'_{\mathcal{S}})$: *(i)* the source location or junction $\ell_{\mathcal{S}} \in Loc_{\mathcal{S}} \cup Junc_{\mathcal{S}}$ and the target location or junction $\ell'_{\mathcal{S}} \in Loc_{\mathcal{S}} \cup Junc_{\mathcal{S}}$, *(ii)* the guard, given by a constraint $Guard_{\mathcal{S}}$, must be satisfied for a transition to be taken, *(iii)* the update, given by a mapping $Update_{\mathcal{S}}$, defines which variables in $Var_{\mathcal{S}}$ are modified, and to what value (unmodified variables keep their value), and *(iv)* the priority, given by $TP_{\mathcal{S}}$, is a natural number between 1 and $od(\ell_{\mathcal{S}})$—the outdegree of (number of transitions leaving) the state or junction $\ell_{\mathcal{S}}$—that indicates the order in which transitions are taken if more than one is enabled.

Simulating an SLSF diagram produces a simulation trajectory, which is closely related to a trajectory of a hybrid automaton.

Definition 4 (*Simulation trajectory*) For an initial state x_0, a time bound $\mathcal{T}_{\max}$, error bound $\delta \geq 0$, and time step $\tau > 0$, a *simulation trajectory* (of length k) is a sequence $\alpha \triangleq ((R_i, t_i))_{i=1\ldots k}$, where $R_0 = \{x_0\}$, $t_0 = 0$, $R_i \subseteq \mathbb{R}^n$, $t_i \in \mathbb{R}^{\geq 0}$, and *(a)* $\forall i : 0 \leq t_{i+1} - t_i \leq \tau$, $t_k = \mathcal{T}_{\max}$, *(b)* $\forall i\ \forall t \in [t_i, t_{i+1}]$: the simulation state after time t is in R_i, and *(c)* $\forall i : dia(R_i) \leq \delta$.

Here $dia(\cdot)$ denotes the diameter and δ is used to bloat the simulation trajectory to handle numerical errors; picking $\delta = 0$ represents the typical result of a (idealized) numerical simulation of an SLSF diagram. We note that the various actions (e.g., `entry`, `during`, and `exit` actions, and transition updates) are evaluated sequentially, while hybrid automaton actions are executed concurrently. By $\mathrm{Trac}_{\delta}(\mathcal{S})$, we denote the set of all simulation trajectories of an SLSF diagram $\mathcal{S}$ with parameter δ. A simulation trajectory α *satisfies* a safety specification P if every element $\alpha.R_i \subseteq P$, i.e., P contains the states of the simulation trajectory with time projected away. An SLSF diagram $\mathcal{S}$ *satisfies* a safety specification P if all simulation trajectories $\mathrm{Trac}_{\delta}(\mathcal{S})$ satisfy P. Note that in practice, any simulation trajectory is finite-length, although we avoid a finite-length assumption in the definition of simulation trajectories to relate possibly infinite trajectories of a hybrid automaton with similar possibly infinite simulation trajectories. Moreover, note that our definition of a trajectory does not allow instantaneous location switches in the hybrid automaton. This restriction is necessary for practical purposes because SLSF requires executing a (small) simulation step in each state.

3 Translating a hybrid automaton to a continuous-time Stateflow diagram

We describe our main contribution, namely how to translate from a hybrid automaton to an SLSF diagram. For different classes of hybrid automata, different translations may be used, and we discuss two classes primarily based on whether the hybrid automaton is deterministic or not.

To compare simulation trajectories of an SLSF diagram with trajectories of a hybrid automaton, we introduce the concept of correspondence. Here, we assume that the δ parameter of a simulation trajectory is equal to zero.

Definition 5 (*Correspondence*) A trajectory ρ of a hybrid automaton $\mathcal{H}$ and a simulation trajectory α (with $\delta = 0$) of an SLSF diagram $\mathcal{S}$ *correspond* to each other if the sequences of discrete locations, transitions, and transition times encountered in both are the same, and the continuous points of the trajectory and the simulation trajectory match.

The primary goal of our construction is to ensure that the set of simulation trajectories $\mathrm{Trac}_\delta(\mathcal{S})$ for the SLSF diagram can be *trajectory-equivalent* to the original hybrid automaton.

Definition 6 (*Trajectory equivalence*) An SLSF diagram $\mathcal{S}$ is *trajectory-equivalent* to a hybrid automaton $\mathcal{H}$ if, for every trajectory ρ of $\mathcal{H}$, there exists a corresponding (Definition 5) simulation trajectory α of $\mathcal{S}$, and for every simulation trajectory α of $\mathcal{S}$, there exists a corresponding trajectory ρ of $\mathcal{H}$.

3.1 Translating different classes of hybrid automata

As already outlined in Sect. 1, one main difference between hybrid automata and SLSF diagrams is the absence of *nondeterminism* in SLSF diagrams. There are several sources of nondeterminism in the general hybrid automaton formalism.

1. *Transitions*. If there is more than one outgoing transition in a location, any of them can be taken as long as the guard is enabled and the target location's invariant is satisfied after applying the transition update.
2. *Dwell times*. The amount of time that a hybrid automaton remains in a location is only determined by the invariant and the transition guards—it is forced to leave the location *only* by the invariant. It is not sufficient for the guard to be enabled at *some* point in time, as the automaton can still choose to remain in the location until the invariant becomes false.
3. *Initial states*. A hybrid automaton is allowed to start in a whole region, which may be an uncountable number of possible initial states.
4. *Updates*. Updates in transitions may be nondeterministic. This gives a (possibly uncountable) number of successor states after a discrete transition.
5. *Flows*. Flow definitions in locations may be uncertain. We do not consider this source of nondeterminism in this paper.

For the translations, we make the following assumptions on the original hybrid automaton.

Assumption 1 The hybrid automaton $\mathcal{H}$ is Zeno-free, which means that only finitely many discrete transitions may be taken in finite time.

Translating deterministic hybrid automata is fairly straightforward, so we first discuss how to translate deterministic hybrid automata and then discuss the more complex nondeterministic scenario. There may be additional numerical issues with SLSF that are outside the scope of this work. For example, the integration of the differential equations in SLSF may not be exact, which may cause differences in observed behavior. In practice, simulations can be made arbitrarily accurate by reducing the simulation time step at a computational cost.

3.1.1 Translating a deterministic hybrid automaton

The next definition states when a hybrid automaton is deterministic.

Definition 7 A hybrid automaton $\mathcal{H}$ is *deterministic* if, for any initial state $(\ell, x_0) \in \mathcal{S}_{init}$ for any point $x_0 \in Init(\ell)$, there is one unique trajectory ρ starting from (ℓ, x_0). Otherwise, $\mathcal{H}$ is *nondeterministic*.

Syntactic restrictions may be enforced on a hybrid automaton to ensure it is deterministic. For example, a sufficient condition for a hybrid automaton to be deterministic includes all of the following being satisfied: (1) at most one discrete transition is enabled simultaneously, (2) a discrete transition guard is enabled when the continuous flow exits the invariant, and (3) no state can be mapped onto two different states by the transition updates [26, Lemma 2]. Note that requirement (2) is not an urgent definition of semantics, but it is a condition that ensures an enabled transition is forced to occur once it becomes enabled, so it is in essence a syntactic restriction that enforces urgency.

Under such assumptions that enforce a hybrid automaton to be deterministic, the translation from the deterministic hybrid automaton to an SLSF diagram is straightforward and proceeds as follows. Let $\mathcal{S} = (Loc_{\mathcal{S}}, Junc_{\mathcal{S}}, Var_{\mathcal{S}}, Trans_{\mathcal{S}}, Actions_{\mathcal{S}})$ be the SLSF diagram. Instantiate $Loc_{\mathcal{S}} = \mathcal{H}.Loc$, $Junc_{\mathcal{S}} = \emptyset$, and $Var_{\mathcal{S}} = \mathcal{H}.Var$. For each location $\ell \in Loc$ and each corresponding location $\ell_{\mathcal{S}} \in Loc_{\mathcal{S}}$, and for each variable $v \in Var$ and the corresponding variable $v_{\mathcal{S}} \in Var_{\mathcal{S}}$, we set the $Actions_{\mathcal{S}}(\ell_{\mathcal{S}}, v_{\mathcal{S}})$ `during` action for $v_{\mathcal{S}}$ to be equal to the flow $\mathit{Flow}(\ell, v)$ for variable v, and do not instantiate the `entry` and `exit` actions. For continuous-time Stateflow models, the `during` action is used to specify an ordinary differential equation for variables, so in essence this just copies the flow from $\mathcal{H}$ to $\mathcal{S}$ for each location and each variable, and the other action types (`entry` and `exit`) are unused.

Finally, we instantiate the transitions as follows. For each location $\ell \in Loc$ and corresponding location $\ell_{\mathcal{S}} \in Loc_{\mathcal{S}}$, and for each transition $(\ell, g, \upsilon, \ell') \in Trans$ with a natural number i indicating the iteration count over the transitions, we instantiate a transition $\gamma \in Trans_{\mathcal{S}}$ as the tuple $(\ell_{\mathcal{S}}, Guard_{\mathcal{S}}, Update_{\mathcal{S}}, TP_{\mathcal{S}}, \ell'_{\mathcal{S}})$, where $\gamma.\ell_{\mathcal{S}} = \ell$, $\gamma.Guard_{\mathcal{S}} = g$, $\gamma.Update_{\mathcal{S}} = \upsilon$, $TP_{\mathcal{S}} = i$, and $\gamma.\ell'_{\mathcal{S}} = \ell'$. Since $\mathcal{H}$ is deterministic, the choice of the transition priority $TP_{\mathcal{S}}$ is unimportant as only at most one transition is enabled

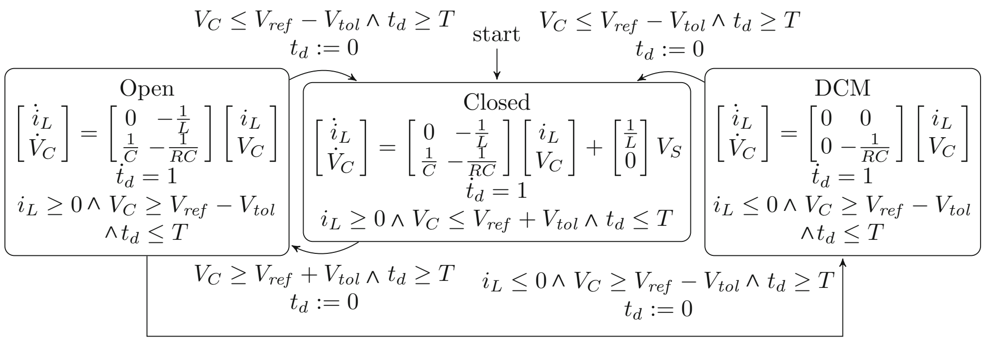
$V_C \leq V_{ref} - V_{tol} \wedge t_d \geq T$
$t_d := 0$
start
$V_C \leq V_{ref} - V_{tol} \wedge t_d \geq T$
$t_d := 0$
Open
$\begin{bmatrix} \dot{i}_L \\ \dot{V}_C \end{bmatrix} = \begin{bmatrix} 0 & -\frac{1}{L} \\ \frac{1}{C} & -\frac{1}{RC} \end{bmatrix} \begin{bmatrix} i_L \\ V_C \end{bmatrix}$
$\dot{t}_d = 1$
$i_L \geq 0 \wedge V_C \geq V_{ref} - V_{tol} \wedge t_d \leq T$
Closed
$\begin{bmatrix} \dot{i}_L \\ \dot{V}_C \end{bmatrix} = \begin{bmatrix} 0 & -\frac{1}{L} \\ \frac{1}{C} & -\frac{1}{RC} \end{bmatrix} \begin{bmatrix} i_L \\ V_C \end{bmatrix} + \begin{bmatrix} \frac{1}{L} \\ 0 \end{bmatrix} V_S$
$\dot{t}_d = 1$
$i_L \geq 0 \wedge V_C \leq V_{ref} + V_{tol} \wedge t_d \leq T$
DCM
$\begin{bmatrix} \dot{i}_L \\ \dot{V}_C \end{bmatrix} = \begin{bmatrix} 0 & 0 \\ 0 & -\frac{1}{RC} \end{bmatrix} \begin{bmatrix} i_L \\ V_C \end{bmatrix}$
$\dot{t}_d = 1$
$i_L \leq 0 \wedge V_C \geq V_{ref} - V_{tol} \wedge t_d \leq T$
$V_C \geq V_{ref} + V_{tol} \wedge t_d \geq T$
$t_d := 0$
$i_L \leq 0 \wedge V_C \geq V_{ref} - V_{tol} \wedge t_d \geq T$
$t_d := 0$

Fig. 3 Composed hybrid automaton model of the closed-loop feedback control system for the buck converter. The buck converter plant is originally modeled as a hybrid automaton, and the hysteresis controller is modeled as a timed automaton (see Fig. 11)

at a time, so it is in essence set arbitrarily to i based on whatever iteration order is chosen. Additionally, the restriction on guards and invariants to ensure determinism means the invariant translation is naturally handled through the translation of the guard as described above.

There are some additional minor syntactic translations that also must occur which we discuss briefly. The first is due to the fact that updates in SLSF are evaluated sequentially, whereas in a hybrid automaton they are evaluated concurrently, so additional temporary variables are introduced to handle this as necessary (e.g., the hybrid automaton update $x' := x + 1 \wedge y' := x$ is rewritten to the SLSF update $x'_{tmp} := x; x' := x_{tmp} + 1; y' := x_{tmp}$, where x_{tmp} is a fresh temporary variable).

The second more significant difference is related to how SLSF identifies events during execution or simulation, which is influenced in part by the simulator not be infinitely precise and have numerical errors. In particular, this influences event detection such as when transitions are enabled and may be taken, and this is implemented using zero-crossing detection algorithms inside the simulation routines of SLSF.

In particular, if a guard is only enabled at one (singular) point in time, it will almost surely not be detected by the zero-crossing mechanisms used by SLSF, and the transition is usually missed. In order to not exclude certain behaviors systematically, we consider an ε-relaxation of each guard constraint, similar to the relaxations considered in translations from SLSF to hybrid automata [30]. For instance, a guard constraint of the form $x = c \wedge y \leq x$ becomes $c - \varepsilon \leq x \leq c + \varepsilon \wedge y \leq x - \varepsilon$. The simulation time step can then be chosen small enough such that, based on the value of ε and the Lipschitz constant of the dynamics, no transitions will be missed.

Although this may permit more behaviors than the original hybrid automaton, it critically prevents transitions from being missed, which is necessary for trajectory equivalence. The extra behaviors introduced from this necessary step can be reduced by considering smaller values of ε, which will require a smaller simulation time step. Reducing the time step, however, will be at the cost of additional simulation runtime.

Example translation We illustrate the translation process with a running case study evaluated in more detail later (Sect. 4.1). A deterministic hybrid automaton for this example appears in Fig. 3, which is a model of a closed-loop control system. Specifically, here a periodically updated hysteresis controller is used to regulate a voltage V_C by controlling the state of a switch. This is a flattened (composed) model of the closed-loop system, originally consisting of a timed automaton model of the hysteresis controller which has periodic updates every 20 microseconds, and a hybrid automaton model with affine dynamics of the plant, which is a circuit known as a buck converter. The resulting continuous-time SLSF diagram for the buck converter created using our translator appears in Fig. 4 (with no ε-relaxations).

3.1.2 Translating a nondeterministic hybrid automaton

For a nondeterministic hybrid automaton, we achieve trajectory equivalence by replacing nondeterminism in the hybrid automaton by (uniformly distributed) random number generation in the SLSF diagram. In this way, by executing multiple SLSF simulations we can approximate the reachable states of the original hybrid automaton.

In our converter, we currently support initial regions and nondeterministic updates to hyper-rectangles, as well as deterministic updates which can be arbitrary functions. When nondeterministic assignments or initial regions are used, they must be strict subsets of the invariant of the target or initial location, respectively, which we note can be statically checked. Under this assumption, the choice of the initial continuous state and the nondeterminism possible during updates can be done by randomly choosing one point from the set of all points available.

In the rest of this section, we focus on the harder problem of nondeterminism from the transitions and the dwell time. We first give an overview of the translation scheme. Here

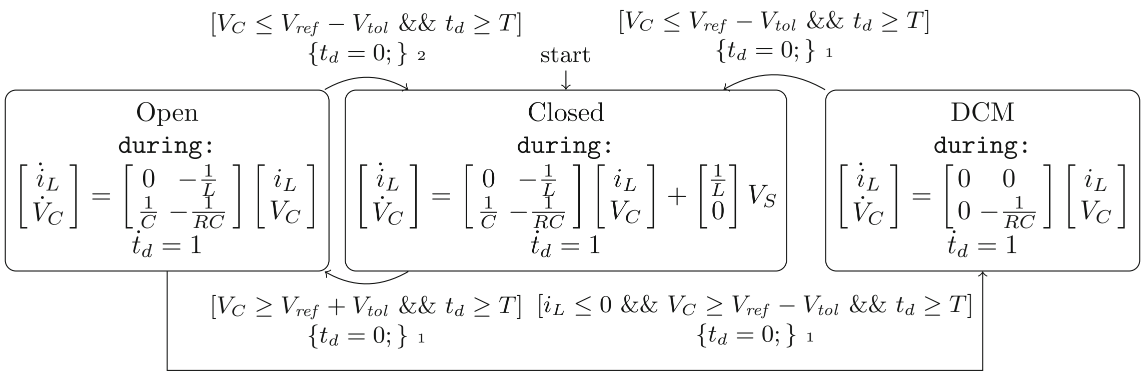
$[V_C \le V_{ref} - V_{tol}\ \&\&\ t_d \ge T]$ $\{t_d = 0;\}$ 2
start
$[V_C \le V_{ref} - V_{tol}\ \&\&\ t_d \ge T]$ $\{t_d = 0;\}$ 1
Open during: $\begin{bmatrix}\dot{i}_L\\ \dot{V}_C\end{bmatrix} = \begin{bmatrix}0 & -\frac{1}{L}\\ \frac{1}{C} & -\frac{1}{RC}\end{bmatrix}\begin{bmatrix}i_L\\ V_C\end{bmatrix}$ $\dot{t}_d = 1$
Closed during: $\begin{bmatrix}\dot{i}_L\\ \dot{V}_C\end{bmatrix} = \begin{bmatrix}0 & -\frac{1}{L}\\ \frac{1}{C} & -\frac{1}{RC}\end{bmatrix}\begin{bmatrix}i_L\\ V_C\end{bmatrix} + \begin{bmatrix}\frac{1}{L}\\ 0\end{bmatrix}V_S$ $\dot{t}_d = 1$
DCM during: $\begin{bmatrix}\dot{i}_L\\ \dot{V}_C\end{bmatrix} = \begin{bmatrix}0 & 0\\ 0 & -\frac{1}{RC}\end{bmatrix}\begin{bmatrix}i_L\\ V_C\end{bmatrix}$ $\dot{t}_d = 1$
$[V_C \ge V_{ref} + V_{tol}\ \&\&\ t_d \ge T]$ $\{t_d = 0;\}$ 1
$[i_L \le 0\ \&\&\ V_C \ge V_{ref} - V_{tol}\ \&\&\ t_d \ge T]$ $\{t_d = 0;\}$ 1

Fig. 4 Composed SLSF diagram for the translated closed-loop feedback control system for the buck converter

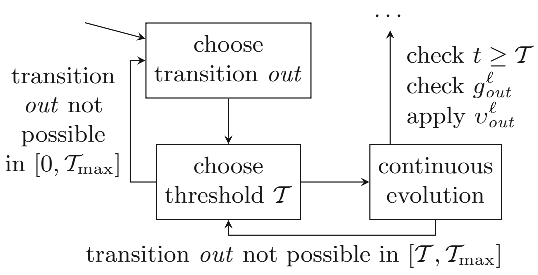
choose transition *out*
transition *out* not possible in $[0, \mathcal{T}_{\max}]$
choose threshold $\mathcal{T}$
continuous evolution
. . .
check $t \ge \mathcal{T}$
check g^{ℓ}_{out}
apply v^{ℓ}_{out}
transition *out* not possible in $[\mathcal{T}, \mathcal{T}_{\max}]$

Fig. 5 High-level location cluster translation pattern consisting of three phases. The location cluster $\hat{\ell}$ denotes a group of SLSF states and junctions which reflects the behavior of the hybrid automaton in the location ℓ

it is helpful to regard the trajectory of a hybrid automaton as a sequence of jumps, and after each jump, the automaton chooses the next transition and dwell time. The crucial difference in our conversion is that the choices might be infeasible, i.e., violating the invariant. To account for this, we incorporate a backtracking mechanism, where the current state of all variables is stored when entering a new location. Note that *time* is an entity which is implicitly present in all hybrid automaton models and we can always add a (fresh) time variable t with flow $\dot{t} = 1$. This allows for a general translation scheme without further knowledge about the hybrid automaton under consideration.

We translate a hybrid automaton location ℓ into a corresponding *location cluster* $\hat{\ell}$, comprising of a number of SLSF states, junctions, and transitions. The clusters are then connected by the same transitions as in the original hybrid automaton. A simulation trajectory of the resulting SLSF diagram then visits those clusters. Inside a cluster, the execution consists of three *phases*, as depicted in Fig. 5.

Three phases in a location cluster In the first phase, we *randomly* choose a transition *out* from the transitions currently available. In the second phase, we choose a time threshold $\mathcal{T}$. In the final phase, we incorporate the original continuous dynamics of the location ℓ.

In the translated model, the transition tries to be taken by checking the original guard condition, but only after dwelling in $\hat{\ell}$ for at least until time moment $\mathcal{T}$. If the transition *out* cannot be taken—possibly due to an invariant violation—in the time frame $[\mathcal{T}, \mathcal{T}_{\max}]$, where $\mathcal{T}_{\max}$ is the maximum simulation time, we *backtrack*[1] and return to the second phase, and select a new time threshold $\mathcal{T}$ which is strictly less than the previously chosen threshold. To ensure termination, we bound the number of times backtracking may occur before trying $\mathcal{T} = 0$. If the chosen transition can still not be taken, we can conclude that it cannot be taken at all, and go back to the first phase, this time trying another transition.

3.2 Trajectory equivalence

The translation process described above maintains the defined notion of trajectory equivalence. For this, we consider an idealized conversion, where there are no numerical errors in the simulation, the value of ε is zero, and the SLSF diagram encodes the intended semantics of the described transformation process.

Theorem 1 *If $\mathcal{H}$ is a Zeno-free hybrid automaton and $\mathcal{S}$ is the* SLSF *diagram created using our transformation process, then $\mathcal{S}$ is trajectory-equivalent to $\mathcal{H}$.*

The proof for the more complex nondeterministic case is given in Sect. 3.3.4. From the theorem, we can conclude that our translation preserves safety properties.

Corollary 1 *If a Zeno-free hybrid automaton $\mathcal{H}$ satisfies a safety specification P, then every simulation trajectory of the translated* SLSF *diagram $\mathcal{S}$ satisfies P.*

[1] We note that our notion of backtracking is different from the one that occurs with multiple junctions in SLSF. In particular, we require allowing some dwell time to elapse in states, whereas junctions are instantaneous.

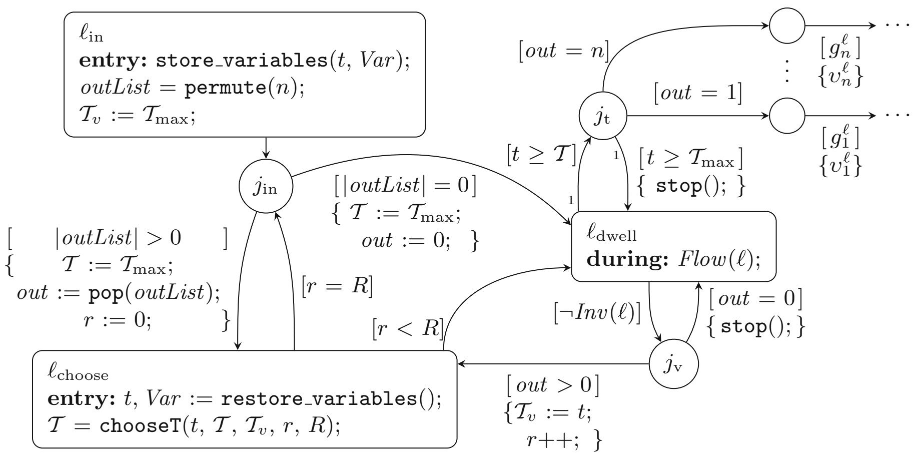
ℓ_{in}
entry: store_variables(t, Var);
$outList$ = permute(n);
$\mathcal{T}_v := \mathcal{T}_{\max}$;
j_{in}
$[\,|outList| = 0]$ $\{\mathcal{T} := \mathcal{T}_{\max}; out := 0;\}$
$[\,|outList| > 0]$ $\{\mathcal{T} := \mathcal{T}_{\max}; out :=$ pop$(outList)$; $r := 0;\}$
$[r = R]$
$[r < R]$
ℓ_{choose}
entry: t, Var := restore_variables();
$\mathcal{T}$ = chooseT$(t, \mathcal{T}, \mathcal{T}_v, r, R)$;
$[out > 0]$ $\{\mathcal{T}_v := t; r{+}{+};\}$
j_{v}
$[\neg Inv(\ell)]$
$[out = 0]$ $\{$ stop(); $\}$
ℓ_{dwell}
during: $Flow(\ell)$;
$[t \geq \mathcal{T}]$
1
1
$[t \geq \mathcal{T}_{\max}]$ $\{$ stop(); $\}$
j_{t}
$[out = n]$
$[out = 1]$
$[g_n^\ell]$ $\{v_n^\ell\}$
$[g_1^\ell]$ $\{v_1^\ell\}$
…

Fig. 6 General location cluster of some location ℓ with n outgoing transitions. (re-)store_variables stores and restores the current simulation state (including the time variable t) from when entering the cluster, respectively. permute(n) returns a permuted list *outList* with all integers from 1 to n. pop(*outList*) removes and returns the first element from *outList*. chooseT chooses a new time threshold $\mathcal{T}$. A subscript "1" indicates that a transition has the highest priority among all the outgoing transitions from a state/junction

3.3 Additional translation details and proof

3.3.1 Detailed translator description

We provide a detailed description of our translation. It iteratively converts every location ℓ of a hybrid automaton and its outgoing transitions into an SLSF diagram of location clusters $\hat{\ell}$ in the following way (see Fig. 6). We first describe the data structures we use in our construction. The list *outList* stores the ordering in which the outgoing transitions of the location ℓ are considered in the simulation. The variable *out* keeps track of the currently chosen outgoing transition. The variable $\mathcal{T}_v$ stores the first time moment when the location invariant is violated. $\mathcal{T}_{\max}$ keeps the maximum simulation time, i.e., the simulation is stopped as soon as this bound has been reached. The variable $\mathcal{T}$ stores the time threshold after which the outgoing transition should be taken. The variable R keeps the maximum number of backtrackings we want to allow, whereas r stores the current number of backtrackings in the location cluster $\hat{\ell}$. Finally, the variable t stores the current time that is simulated. Introducing this variable allows us to model going back in time when backtracking, which is not possible for the actual simulation time that is tracked by SLSF.

We continue with the description of every individual (SLSF) state in our construction. The current simulation time and the hybrid automaton state when entering the location ℓ (and, respectively, the location cluster $\hat{\ell}$) is stored in the (SLSF) state ℓ_{in}. Furthermore, the algorithm *randomly* chooses the ordering in which the outgoing transitions are considered. In this way we handle the nondeterminism due to multiple simultaneously enabled transition guards. Finally, the variable $\mathcal{T}_v$ is initialized to $\mathcal{T}_{\max}$ as we do not have any information about the invariant violation at that moment.

The state ℓ_{choose} covers two kinds of nondeterminism. It takes care of the situation when the intersection of the invariant and the transition guard is nonsingular, i.e., when a switch to the next location can happen not only at a particular time moment, but within a *time interval*. Note that if the continuous dynamics are nonmonotonic, there can be multiple *disjoint* time intervals where the guard is enabled. We resolve such situations by generating a *random* time threshold $\mathcal{T}$ in the state ℓ_{choose} and allowing the discrete transition only from the time moment $\mathcal{T}$ onward, i.e., we add a constraint of the form $t \geq \mathcal{T}$ as a part of the transition guard for every outgoing transition from the location ℓ. Thus, we disable the SLSF must-semantics up until time moment $\mathcal{T}$ to mimic the original may-semantics of hybrid automata.

Note that we also use the state ℓ_{choose} for *backtracking* purposes. We observe that an unfortunate choice of the outgoing transition *out* and the time threshold $\mathcal{T}$ can lead to the simulation getting stuck, as the transition guard of *out* is not enabled in the time frame $[\mathcal{T}, \mathcal{T}_{\max}]$, and thus, the transition cannot be taken. In such cases, we return to the state ℓ_{choose} to select a further time threshold $\mathcal{T}$. For this purpose, we restore the simulation time t and the state of the hybrid automaton from the moment we entered ℓ resp. $\hat{\ell}$. Afterward, we can choose the next time threshold from the interval $[t, \mathcal{T}]$. Here we observe that in general before reaching the time threshold, the invariant can be violated. Thus, we actually select a new threshold from the interval $[t, \min(\mathcal{T}, \mathcal{T}_v)]$. In this way, we end up with a sequence of monotonically decreasing thresholds. Still, as it is not guaranteed that the chosen threshold is eventually equal to 0, we add a further termination criterion by bounding the number of backtracking by some user-defined constant $R > 0$. The last time before exceeding this limit, we try out the weakest

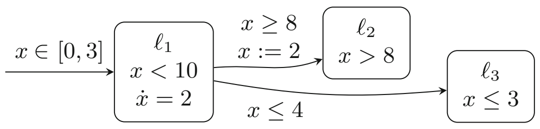

Fig. 7 Snippet of an example hybrid automaton with three locations $\ell_1 - \ell_3$

threshold $\mathcal{T} = 0$ to ensure that we have covered all cases. If the transition cannot be taken at all, we either proceed with a further outgoing transition (junction j_{in}) or, if none is left, the simulation is stopped and reports an actual deadlock in the model.

The continuous evolution corresponding to the location ℓ is modeled by the state ℓ_{dwell}. We can leave this state under two conditions. First, the invariant can be violated. Then, we store the time moment when the violation has happened in the variable $\mathcal{T}_v$ and move to the state ℓ_{choose} (via junction j_{v}). Note that if we have already considered all the outgoing transitions of ℓ, we will stop the simulation since a deadlock has been found. In the other case, the time threshold $\mathcal{T}$ can be reached. We take the transition to the successor location of ℓ if the guard of the chosen transition *out* is enabled and after applying the update, the target location's invariant is satisfied (junction j_{t}). Furthermore, here we also check whether the maximum simulation time $\mathcal{T}_{\max}$ has been reached, in which case we stop the simulation.

In the following, we illustrate the translation process using an example simulation.

3.3.2 Example

We consider an execution in some location cluster for a simple location ℓ_1 with one continuous variable x and two outgoing transitions, as depicted in Fig. 7. For simplicity, assume that the location is entered at time $t = 0$ in state $x = 0$ and the total simulation time is $\mathcal{T}_{\max} = 20$.

First we store the current continuous state $(t, x) = (0, 0)$. Next, in phase 1, we choose a transition, say, the one to ℓ_2. Then, in phase 2, we choose a random minimum dwell time in the range $[0, 20]$, say $\mathcal{T} = 3$. The simulation proceeds in phase 3 until an event occurs. In this case, events are either violating the location invariant $x < 10$ or enabling the guard condition of the selected transition $t \geq 3 \wedge x \geq 8$. The guard condition is enabled first, at state $(t, x) = (4, 8)$. This transition cannot be taken, however, as the target invariant would be violated after applying the update $x := 2$. The simulation continues until the next event, when the state $(t, x) = (5, 10)$ is reached and a violation of the invariant is detected. That is why the simulation goes back to phase 2, backtracking to the saved state $(t, x) = (0, 0)$. At this point, it was checked that for all $\mathcal{T} \geq 3$, the transition cannot be taken. In phase 2, a new value for $\mathcal{T}$ is chosen from the restricted interval $[0, 3)$, and the simulation is run again in phase 3. After reaching the same conclusion and after further backtracking, a finite threshold of attempts is reached, and $\mathcal{T} = 0$ is forced. Even with $\mathcal{T} = 0$, there will be a violation of the invariant before the transition can be taken. Then, we will conclude that the selected transition can never be taken when starting in the state $(t, x) = (0, 0)$. Thus, we can safely ignore this transition, go back to phase 1 and choose the transition leading to ℓ_3, where the process repeats.

3.3.3 Translation correctness and discussion

Correctness The proof of Theorem 1 required three assumptions, mentioned before the theorem statement and proven below. First, we assumed the simulations were exactly accurate. Although real simulations will always have some error, this can be reduced to arbitrarily small values by reducing the time step used in the simulation. Similarly, for the second assumption we can consider smaller and smaller values of ε, although in degenerate cases this might permit extra transitions in the simulation. For example, a degenerate guard like $x < 5 \wedge x > 5$ will always be false, but any positive ε-relaxation will have a possible transition when $5 - \varepsilon < x < 5 + \varepsilon$. The third assumption is that the SLSF diagram correctly encodes the described transformation process. This means that correctness is subject to possible implementation bugs in our conversion implementation in HyST, as well as the semantics of SLSF. In addition to the trajectory equivalence theorem, we provide empirical justification for the correctness of the implementation of our translation scheme, through extensive case studies including the buck converter detailed in the main body, and additional case studies presented later in appendix.

Nondeterminism When replacing nondeterminism with random number generation, some behaviors of the original hybrid automaton might be obscured. For instance, a nondeterministic die can roll a six forever, while the probability of this behavior for a random die approaches zero as more rolls are taken. We always deal with finite executions in a simulation and thus end up with a finite number of choices, so there is still a nonzero chance that the "right" random values will be chosen, assuming that the hybrid automaton is Zeno-free.

Generalizations Although we consider a large class of hybrid automata, further generalizations are possible. For example, the initial sets and nondeterministic resets in our framework were hyper-rectangles, whereas in general, the initial state could be in a nonconvex set, and the reset might be an arbitrary function which maps from a single state to a nonconvex set. To handle such systems, we need a way to sample in the nonconvex destination sets, which may be possible in certain situations, but is difficult in general. One possibility would be to require the user to give this sampling function.

Another possible generalization is to consider nondeterministic dynamics. More general hybrid automata may include differential inclusions or other nondeterministic ways for the continuous states to evolve. This could be handled by adding ranged inputs to the system, and at each time step choosing a random value in the range for each input. However, as the time steps become smaller, the random inputs will approximate the main value in their ranges, which in practice results in poor simulation coverage. An alternative is to choose a time step where the inputs will vary, such that a trade-off is possible between the amount of coverage possible and the effect of this tendency toward the mean. Other simulation methods, perhaps based on state exploration mechanisms such as rapidly exploring random trees (RRTs) [28], may also be possible.

3.3.4 Proof

Proof (Theorem 1) We first show the forward direction, i.e., given an arbitrary trajectory of the hybrid automaton, there exists a set of random decisions in the constructed SLSF diagram that produce a corresponding simulation trajectory.

Recall that correspondence (Definition 5) requires that the encountered locations can be the same and that the deviation in continuous states can be bounded by an arbitrarily small constant.

For the ordering of locations, notice that the random choice of an outgoing transition in phase 1 of the construction can pick the corresponding transition from the trajectory. Since the minimum dwell time is chosen randomly, it can be picked to be arbitrarily close to the dwell time in the hybrid automaton trajectory. In this way, as long as the continuous evolution in the simulation remains close to the hybrid automaton trajectory's continuous evolution, every transition will be explored.

The second part of correspondence requires that the deviation in the continuous states is bounded. We show that this bound can be chosen to be arbitrarily small across both every continuous evolution and after every discrete transition. During a continuous evolution, if the start state in a location in the simulation is chosen close to the start state in the corresponding location in the hybrid automaton trajectory, its deviation will also be bounded as a function of the Lipschitz constant (see Proposition 1 in [19]). Thus, for a single bounded continuous evolution and every nonzero final state deviation desired, there is a corresponding nonzero initial state deviation that will achieve the desired closeness.

During initial state selection, since we consider hyperrectangles, the set of states is bounded. By randomly choosing states, we will, in finite time, pick a state arbitrarily close to any trajectory's start state in the hybrid automaton.

Finally, for updates, the dwell time of a simulation can be made arbitrarily close to a hybrid automaton trajectory, and since the state can be made arbitrarily close, a deterministic update function (under assumptions of Lipschitz continuity) can also result in a state arbitrarily close to the trajectory. For nondeterministic updates, the argument is similar to the initial state selection, and thus, the continuous states of the simulation remain arbitrarily close to the hybrid automaton trajectory.

The sequence of discrete transitions between the trajectory and simulation match. Since each trajectory is a finite sequence of discrete transitions (due to Zeno-free behavior) and continuous evolutions (each of which can have arbitrarily small error between the trajectory and a possible simulation), the accumulated error for the whole trajectory can also be made arbitrarily small. Thus, the constructed SLSF diagram has simulations which correspond to any arbitrary hybrid automaton trajectory.

The reverse direction in the proof shows that any arbitrary simulation has a corresponding hybrid automaton trajectory. Again, we proceed by decomposing this into showing that the sequence of locations is the same, and that the deviation in the continuous state is bounded.

Since we assumed an idealized relaxation where ε is zero, every transition in the simulation exactly matches the guard conditions in the hybrid automaton, and thus, the hybrid automaton can match the simulation. Every update in the constructed SLSF diagram is also copied from the automaton, so that the automaton's trajectory can match the random choices made by a simulation.

For continuous trajectories, the simulation will choose some dwell time where the invariant remains satisfied until a guard becomes true. The hybrid automaton can also pick the same dwell time, and its invariant will also remain true until the same guard condition is reached. Thus, the hybrid automaton can pick a trajectory which corresponds to the simulation.

Since every trajectory of the hybrid automaton corresponds to a simulation trajectory of the SLSF diagram, and every simulation trajectory corresponds to a trajectory, the two models are trajectory-equivalent. □

4 Evaluation and experimental results

To evaluate the translation methodology presented in this paper, we implemented a prototype translator that uses the HyST intermediate representation for source-to-source transformation of hybrid automata [5], and the SLSF API within MATLAB (tested with versions 2014a through 2016a). The input to the translator is a hybrid automaton $\mathcal{H}$ in the

SpaceEx XML format. Networks of hybrid automata are first composed within HyST to yield a single hybrid automaton representing the network. Once parsed in the tool, an object representing the syntactic structure of $\mathcal{H}$ is traversed, and then, the tool applies the sequence of translation steps described in Sect. 3. In the simulator, we varied the seeds of the uniform pseudo-random number generator `rng` in MATLAB. We evaluated the prototype tool using several examples. For this, we first computed the reachable states of the models in SpaceEx or Flow* and then performed the translation and simulations in SLSF. The tool and examples are available for download [24].

4.1 Case study: buck converter with periodic hysteresis controller

A buck converter is a DC-to-DC switched-mode power supply that takes a DC input source voltage and lowers ("bucks") it to a smaller DC output voltage [32]. A standard model of the converter has three modes, where the switch is closed and the voltage source is connected, where the switch is open and the voltage source is disconnected, and based on the possible dynamics of the converter, a third mode, known as the discontinuous conduction mode (DCM), where the current is not allowed to go below zero (which is physically unrealizable, but may occur without this third mode). Interested readers may find detailed derivations of models in power electronics textbooks [41]. A hybrid automaton model of the closed-loop buck converter (plant and timed controller) appears in Fig. 3.

A standard closed-loop controller for the buck converter is a hysteresis controller, which changes the mode of the buck converter plant based on the measured output voltage. Its operation depends on opening and closing the MOSFET switch. Intuitively, it operates like a thermostat, i.e., the switch is toggled so that the source voltage is connected to the circuit if the output voltage is too low, and it is toggled in case if the output voltage is too high to disconnect the voltage source. We note that by Kirchhoff's voltage law (KVL), $V_C = V_{out}$ [41]. In part to avoid switching too frequently, a hysteresis band is typically used so switches occur when $V_{out} \geq V_{ref} + V_{tol}$ or $V_{out} \leq V_{ref} - V_{tol}$. This creates a voltage ripple on the output voltage that should be within a given range V_{rip} of the desired reference output voltage V_{ref}. Together, these define a safety specification: $P(t) \triangleq t \geq t_s \Rightarrow V_{out}(t) = V_{ref} \pm V_{rip}$, which projected onto the phase space is $P \triangleq V_{ref} - V_{rip} \leq V_{out} \leq V_{ref} + V_{rip}$. SpaceEx is used to verify P by computing the reachable states Reach($\mathcal{H}$) (to a fixed-point) from a startup state where the initial states $\mathcal{S}_{init}$ are $i_L = 0$ and $V_C = 0$. For every time $t \geq t_s$ after a startup trajectory of duration t_s, if $V_{ref} - V_{rip} \leq V_{out}(t) \leq V_{ref} + V_{rip}$, then the converter satisfies the specification P.

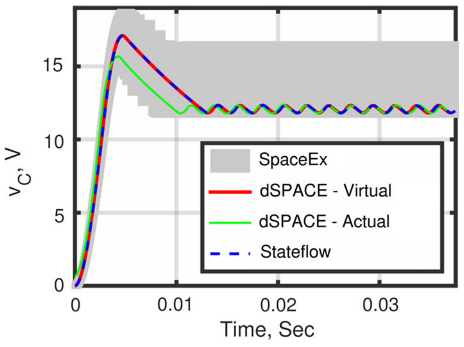

Fig. 8 Reachable states of the hybrid automaton computed with SpaceEx, verifying the voltage-regulation property, along with HiL simulation results of the translated SLSF diagram on the DS1103 ("virtual plant"), and control of the physical plant with the translated SLSF diagram ("actual plant"). Our results validate the high-level vision of correct-by-construction control implementation from Fig. 1

For actual implementations, the measured voltage values are sensed periodically through an analog-to-digital converter (ADC), and subsequently, the control signals are sent periodically to control the state of the buck converter transistor (open/closed). We model this periodic update process as a timed automaton for the controller with a timer variable t_d that evolves at unit rate and is upper bounded by T of 20 microseconds. The reachable states of the closed-loop buck converter hybrid automaton are computed with SpaceEx, and as shown in Fig. 8, the model satisfies the safety specification P for a sufficient choice of V_{rip}.

A hardware setup consisting of a buck converter plant, and a dSpace DS1103 is used to perform the experiments with the physical buck converter plant. The DS1103 contains a Power PC processor and a DSP board and is used for implementation of the hybrid automata in both hardware-in-the-loop (HiL) simulations with a "virtual plant" (the plant model simulated on the DS1103 hardware) and the actual buck converter plant.

The hysteresis controller is executed on the DS1103. First, we generate C code using the translated SLSF diagram in MATLAB, then compile it and download it onto the DS1103. A discrete fixed-step solver with a time step of 20 microseconds is used for the code generation process and also for the DS1103's sampling and control periods, which is sufficiently small to ensure ε is sufficiently small, as discussed in Section 3. The measured voltage signal from the buck converter is periodically sensed and sent to the embedded controller through an ADC. The embedded controller generates Boolean valued signals, and these are converted to suitably spaced rectangular pulses to operate the MOSFET switch of the buck converter plant. For the experiments with the actual plant, the input signals fed to the controller (specifically the V_C voltage) are replaced from the simulation model with the measurement of the actual plant, and the output signals (the desired mode, open or closed) are fed to the

(a)

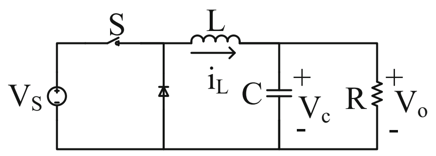

(b)

Component / Parameter Name	Symbol	Value
Source Input Voltage	V_S	24 V
Desired Output (Reference) Voltage	V_{ref}	12 V
Actual Output Voltage	$V_C = V_{out}$	12 V $\pm V_{rip}$
Hysteresis Band Tolerance	V_{tol}	0.1 V
Voltage Ripple Tolerance	V_{rip}	0.6 V
Load Resistance with Parameter Variation	R	$10 \pm 2\%\ \Omega$
Capacitor Value with Parameter Variation	C	$2.2 \pm 2\%$ mF
Inductor Value with Parameter Variation	L	$2.65 \pm 2\%$ mH
Periodic Updation Parameter	T	20 μ sec

Fig. 9 **a** Buck converter circuit—a DC input V_S is decreased to a lower DC output $V_C = V_o = V_{out}$. **b** Buck converter parameter values and variations

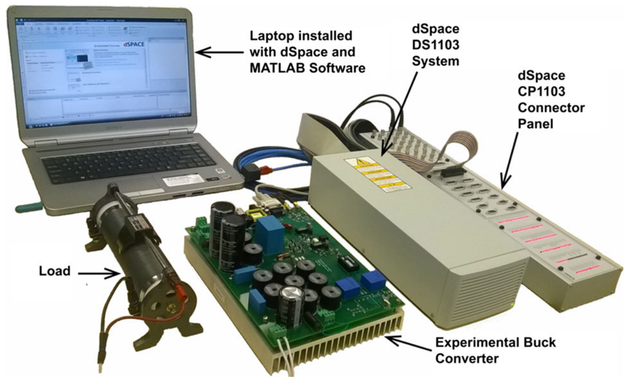
Laptop installed with dSpace and MATLAB Software
dSpace DS1103 System
dSpace CP1103 Connector Panel
Load
Experimental Buck Converter

Fig. 10 Buck converter plant controlled with a dSPACE DS1103 system. Our results controlling the actual plant with the translated controller validate the high-level vision of correct-by-construction control implementation from Fig. 1

actual plant instead of the simulation model. The experimental results are recorded, and a comparison to SLSF simulations is shown in Fig. 8. The experimental and simulation traces are contained in the SpaceEx reach sets, which validates the translation correctness (Theorem 1) and that the safety property is maintained in the implementation (Corollary 1). Note that in the hardware experiments, the controller has essentially been determinized, as the purpose of nondeterminism in the hybrid automaton model was to model plant inaccuracies.

4.1.1 Additional details

The buck converter circuit appears in Fig. 9a. Parameter values used for the case study appear in Fig. 9b.

A hybrid automata network model of the buck converter plant and a timed automaton of the hysteresis controller appears in Fig. 11, where θ is a synchronization label and δ is a discrete control signal, and a bisimilar hybrid automaton model after flattening (composing) the network is shown earlier in Fig. 3. The composed model from Fig. 3 is used for verification, translation, and code generation purposes as discussed earlier, while the network model is conceptually simpler and illustrates the decomposition between the physical plant hardware and the controller. The physical hardware used in the evaluation appears in Fig. 10.

Figure 12 (resp. Fig. 13) shows the reachable states together with a number of simulations. The plots illustrate that the SLSF simulations are contained in the reachable states computed with SpaceEx and give empirical evidence for the correctness of the translation.

4.2 Case study: yaw damper controller for 747 aircraft

A yaw damper is modeled as a multiple-input multiple-output (MIMO) system which uses the aileron and rudder in order to reduce oscillations in the yaw and roll angle of an aircraft. In this section, we use the proposed method to analyze the control design of a yaw damper for a 747 aircraft, taken from the Control Systems Toolbox case studies in MATLAB.

In particular, we analyze the final designed controller, which includes a washout filter capable of eliminating oscillations, but maintaining the spiral mode. The spiral mode is a desired control characteristic in yaw damper systems, where an impulse input from the aileron will result in a bank angle which does not immediately decrease to zero.

The model for the system is given at Mach 0.8 at 40,000 ft using standard linear time-invariant dynamics, $\dot{x} = Ax + Bu$. There are four physical variables in the system $x = (x_1, x_2, x_3, x_4)^T$, which are sideslip angle (x_1), yaw rate (x_2), roll rate (x_3), and bank angle (x_4), represented by the column vector x. The two inputs $u = (u_1, u_2)^T$ are the rudder (u_1) and aileron (u_2). The outputs are the yaw rate and bank angle.

The specific values for A and B are:

$$A = \begin{bmatrix} -0.0558 & -.9968 & 0.0802 & 0.0415 \\ 0.598 & -0.115 & -0.0318 & 0 \\ -3.05 & 0.388 & -0.4650 & 0 \\ 0 & 0.0805 & 1 & 0 \end{bmatrix},$$

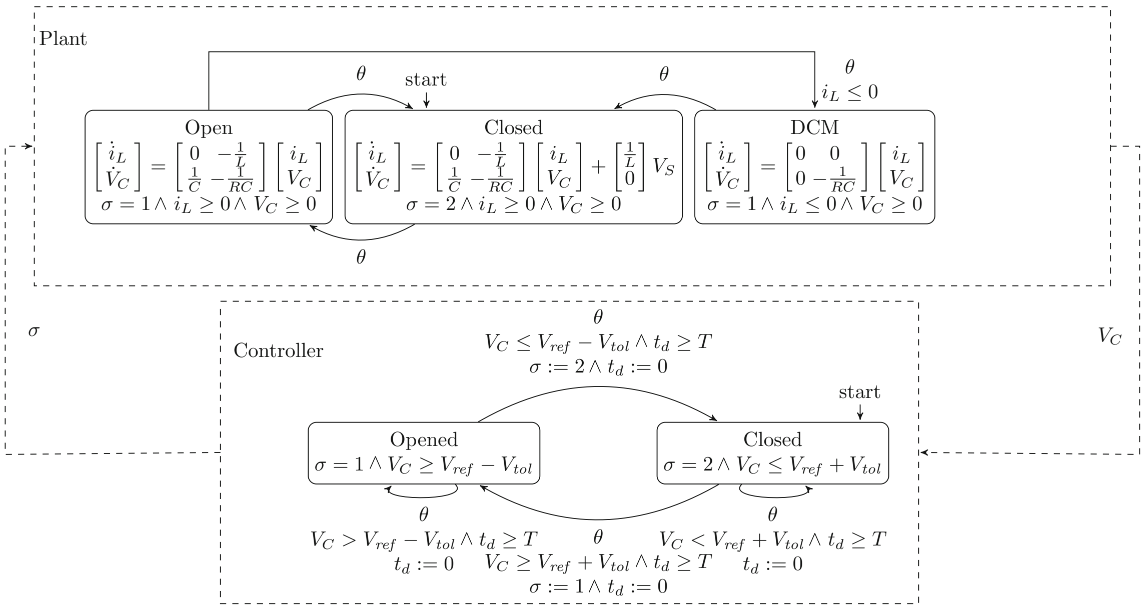
Plant
Open
Closed
DCM
start
θ
$i_L \le 0$
$\begin{bmatrix}\dot{i}_L\\ \dot{V}_C\end{bmatrix} = \begin{bmatrix}0 & -\frac{1}{L}\\ \frac{1}{C} & -\frac{1}{RC}\end{bmatrix}\begin{bmatrix}i_L\\ V_C\end{bmatrix}$
$\sigma = 1 \wedge i_L \ge 0 \wedge V_C \ge 0$
$\begin{bmatrix}\dot{i}_L\\ \dot{V}_C\end{bmatrix} = \begin{bmatrix}0 & -\frac{1}{L}\\ \frac{1}{C} & -\frac{1}{RC}\end{bmatrix}\begin{bmatrix}i_L\\ V_C\end{bmatrix} + \begin{bmatrix}\frac{1}{L}\\ 0\end{bmatrix} V_S$
$\sigma = 2 \wedge i_L \ge 0 \wedge V_C \ge 0$
$\begin{bmatrix}\dot{i}_L\\ \dot{V}_C\end{bmatrix} = \begin{bmatrix}0 & 0\\ 0 & -\frac{1}{RC}\end{bmatrix}\begin{bmatrix}i_L\\ V_C\end{bmatrix}$
$\sigma = 1 \wedge i_L \le 0 \wedge V_C \ge 0$
σ
V_C
Controller
$V_C \le V_{ref} - V_{tol} \wedge t_d \ge T$
$\sigma := 2 \wedge t_d := 0$
Opened
$\sigma = 1 \wedge V_C \ge V_{ref} - V_{tol}$
Closed
$\sigma = 2 \wedge V_C \le V_{ref} + V_{tol}$
$V_C > V_{ref} - V_{tol} \wedge t_d \ge T$
$t_d := 0$
$V_C \ge V_{ref} + V_{tol} \wedge t_d \ge T$
$\sigma := 1 \wedge t_d := 0$
$V_C < V_{ref} + V_{tol} \wedge t_d \ge T$
$t_d := 0$

Fig. 11 Hybrid automaton model of the buck converter plant with timed automaton of the hysteresis controller as a network

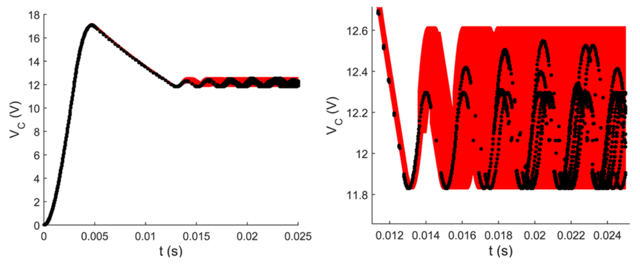

Fig. 12 *Left* Buck converter V_C versus time, with SpaceEx reach set for the hybrid automaton model in *red*, and *black* points from 10 simulation traces of the translated SLSF diagram. *Right* Detailed and zoomed view illustrating multiple simulation trajectories (color figure online)

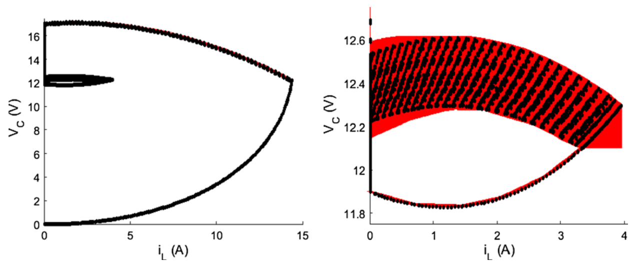

Fig. 13 *Left* Buck converter V_C versus i_L (phase space), with SpaceEx reach set in *red*, and *black points* from 100 simulation traces. *Right* Detailed and zoomed view illustrating multiple simulation trajectories (color figure online)

$$B = \begin{bmatrix} .00729 & 0 \\ -0.475 & 0.00775 \\ 0.153 & 0.143 \\ 0 & 0 \end{bmatrix}$$

This physical system is put into a feedback loop with a washout filter, which has a single variable w and dynamics $\dot{w} = x_2 - 0.2 \cdot w$. The filter variable is combined with the yaw to produce an effect on the rudder input. In particular, the washout filter adds to u_1 the value $2.34 \cdot (x_2 - 0.2 \cdot w)$.

We consider analysis of a system model which has the guarantees given by a real-time scheduler, which periodically executes the washout filter and sets the output values. Between controller executions, we take the output of the washout filter to be constant (zero-order hold). The control task is guaranteed to execute every period using a common scheduler like Rate Monotonic (RM) or Earliest Deadline First (EDF). There is nondeterminism in the exact time the controller runs, however, due to the offset of the execution of the control task within each period. Since the control logic is simple, we take the control task to be nonpreemptive and short, so that the model will sample the physical system and update the filter output at a single point in time, but that point in time may vary within each period. Furthermore, we look at the system response due to an impulse input from the aileron from a range of start conditions. We take the initial bank angle to be between 0 and 0.1.

This system was modeled in SpaceEx, and reachability analysis was attempted in both SpaceEx and Flow*. Due to the large number of discrete switches, however, neither tool is able to directly compute reachability (the computed reach sets grow exponentially).

Instead, we investigate the system using our conversion to SLSF and randomized execution. Since the main source of nondeterminism in this model is the discrete switches, we can investigate simulations of the system where they occur at varying offsets from the start of each period.

The simulations showed the expected response of the system when using a controller period of $T = 0.1$. The response of the system is shown in Fig. 14. Here, the impulse response from the aileron to the bank angle is plotted, which does not immediately converge (spiral mode), and does not contain excessive oscillations. Thus, using the technique proposed in this paper we are able to analyze a system which cannot be directly analyzed using reachability tools.

This system can be analyzed formally; however, this requires a nontrivial model transformation using the technique of continuization, as well as using a smaller control period. Continuization converts the periodically actuated model into a continuous one with bounded noise, where the bound is based on the controller period and maximum rate of change of the output signal [6]. The same model can be used as the basis for the conversion using continuization, as well as the conversion to SLSF for simulation and further MATLAB-based analysis and code generation. In this way, the conversion to SLSF is one part of a larger toolflow, where models are first created in SpaceEx, possibly converted for formal analysis using HyST and then can be directly imported into SLSF after the conversion described in this paper for simulation and controller synthesis, as well as embedding in a larger CPS model.

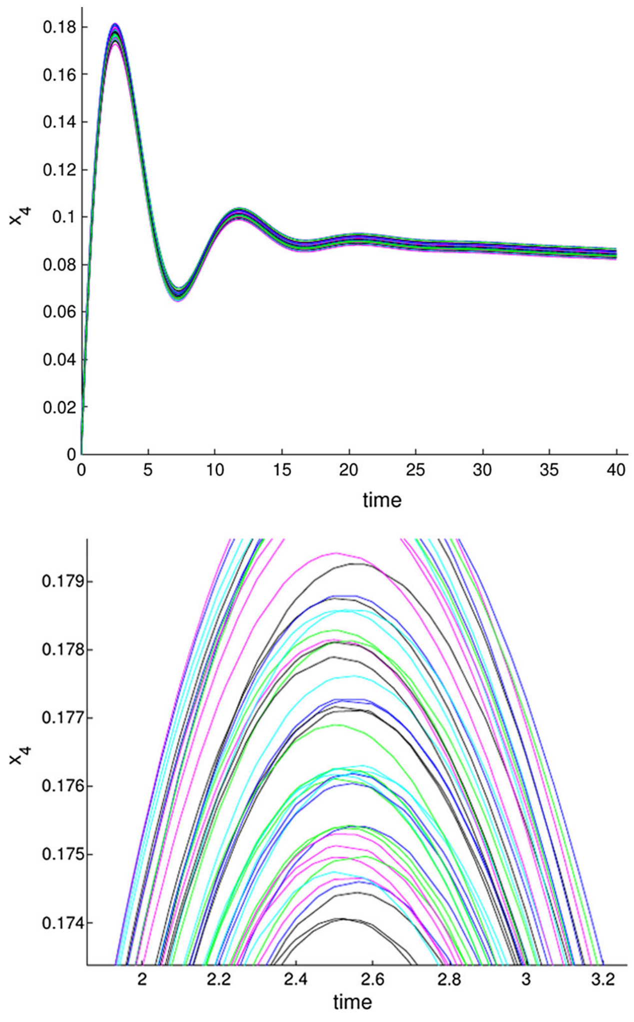

Fig. 14 Fifty simulations of the yaw damper system. *Top* The spiral mode is confirmed. *Bottom* Nondeterminism in controller execution time causes simulated trajectories to cross

4.3 Case study: glycemic control in diabetics

Glycemic control is an approach to control the blood glucose levels in insulin-dependent diabetes mellitus patients. There are several different mathematical models of glycemic control used to design insulin infusion devices that help diabetic patients control their blood glucose levels [20]. Here we investigate a nonlinear hybrid system of the glycemic control in diabetic patients such that all dynamics are defined by polynomials. The mathematical model is described by the following ODEs:

$$\dot{G} = -0.01G - X(G + G_B) + g(t) \tag{1}$$
$$\dot{X} = -0.025X + 0.000013I \tag{2}$$
$$\dot{I} = -0.093(I + I_B) + u(t)/12 \tag{3}$$

In Eqs. 1 and 3, G and I are the plasma glucose concentration and the plasma insulin concentration above their basal value G_B and I_B, which are equal to 4.5 and 15, respectively. The variable X shown in Eq. 2 is the insulin concentration in an interstitial chamber. Moreover, $g(t)$ and $u(t)$ are the influx of glucose and the insulin control input, presented in Eqs. 4 and 5, respectively.

$$g(t) = \begin{cases} t/60 & \text{if } t \le 30 \\ (120 - t)/180 & \text{if } 30 < t \le 120 \\ 0 & \text{if } t > 120 \end{cases} \tag{4}$$

$$u(t) = \begin{cases} 25/3 & \text{if } G(t) \le 4 \\ 25/3(G(t) - 3) & \text{if } 4 < G(t) \le 8 \\ 125/3 & \text{if } G(t) > 8 \end{cases} \tag{5}$$

The glycemic control was first modeled in SpaceEx and then translated to Flow* by using the HyST model converter. This model is nonlinear, nondeterministic, and includes four variables, nine locations, and 18 discrete transitions in total. The simulations of the glycemic control model translated to SLSF are shown in Fig. 15. We simulated the translated model with 100 different randomized executions. All simulation traces of G are contained in the reach set computed by Flow*, which validates the translation.

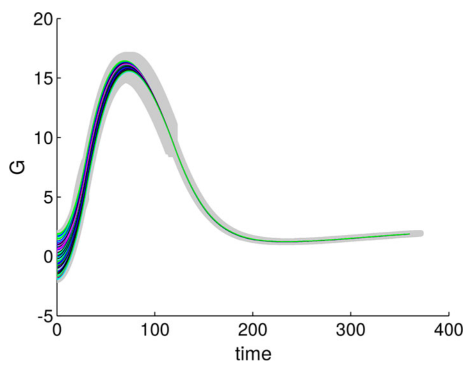

Fig. 15 One hundred simulations of the glycemic control model with simulations and reach set computed by Flow* (*gray*) for variable G

4.4 Case study: Fischer mutual exclusion

Fischer mutual exclusion is a timed distributed algorithm that ensures a mutual exclusion safety property, namely that at most one process in a network of N processes may enter a critical section simultaneously. An automaton for Fischer appears in Fig. 16. Fischer involves two real timing parameters, A and B, and mutual exclusion is ensured iff $A < B$.

Let $Loc \triangleq \{rem, try, waits, cs\}$. We translated a network of two automata ($N = 2$) from SpaceEx to SLSF. In one instance, we ensured $A < B$ by picking $A = 5$ and $B = 70$, so mutual exclusion was maintained, which we verified in SpaceEx using the PHAVer scenario. In the other instance, we ensured $A > B$ by picking $A = 75$ and $B = 70$, and mutual exclusion was not maintained. Consequently, we could not verify this instance using SpaceEx's PHAVer scenario since a location $cs \sim cs$ was reachable, corresponding to the case where both processes are in the critical section. We conducted $K = 1000$ simulations with maximum time $T = 1000s$ of the translated SLSF model in each case. In Fig. 17, we show, respectively, the property satisfaction and violation through the automatic translation from SpaceEx to SLSF by plotting the corresponding locations versus time, where different colors correspond to different simulations. In the safe case ($A < B$), all the locations reached via simulations did maintain the mutual exclusion property and were $Loc^2 \setminus \{cs \sim cs, try \sim cs, cs \sim try\}$. In the unsafe case ($A > B$), the locations reached via simulation included every location (e.g., all 16 locations of the permutations of Loc^N for $N = 2$) and violated the mutual exclusion property. These results give further empirical evidence for the correctness of the translation procedure.

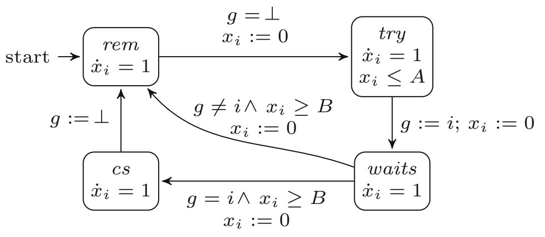
$$\begin{tikzcd}
\text{start} \arrow[r] & \begin{matrix} rem \\ \dot{x}_i = 1 \end{matrix} \arrow[rr, "\begin{matrix} g = \bot \\ x_i := 0 \end{matrix}"] & & \begin{matrix} try \\ \dot{x}_i = 1 \\ x_i \le A \end{matrix} \arrow[d, "g := i;\ x_i := 0"] \\
& \begin{matrix} cs \\ \dot{x}_i = 1 \end{matrix} \arrow[u, "g := \bot"] & & \begin{matrix} waits \\ \dot{x}_i = 1 \end{matrix} \arrow[ll, "\begin{matrix} g = i \wedge x_i \ge B \\ x_i := 0 \end{matrix}"] \arrow[ull, bend right, "\begin{matrix} g \ne i \wedge x_i \ge B \\ x_i := 0 \end{matrix}"']
\end{tikzcd}$$

Fig. 16 Fischer's mutual exclusion algorithm for a process with identifier $i \in \{1, \ldots, N\}$. Here, g is a global variable of type $\{\bot, 1, \ldots, N\}$, x_i is a local variable of type $\mathbb{R}$, and both A and B are constants of type $\mathbb{R}$

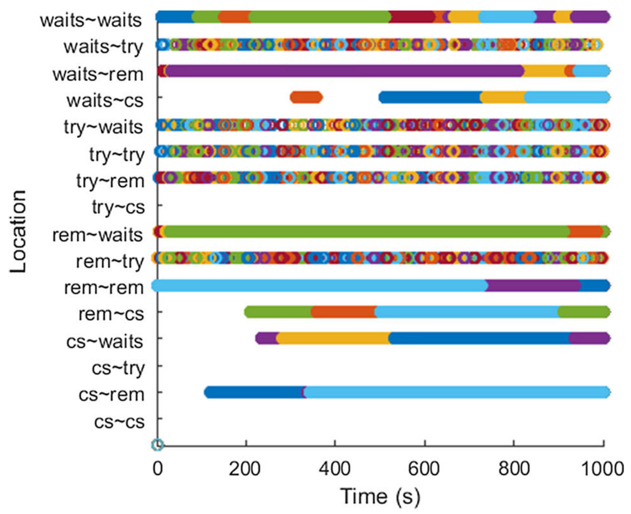

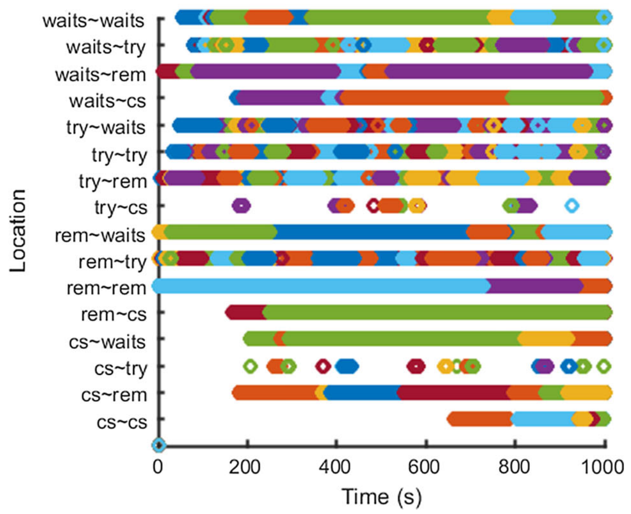

Fig. 17 Locations reached for 1000 SLSF simulations of Fischer, where different colors indicate different trajectories. *Top* safe case. *Bottom* unsafe case

4.5 Additional case studies

Table 1 summarizes the different types of benchmarks that were all successfully translated and checked for trajectory equivalence in addition to the previously presented case studies. The experiments were performed on an Intel I5 2.4 GHz machine with 8 GB RAM. All benchmarks are available in supplementary material [24].

Table 1 Overview of the benchmark problems successfully translated to SLSF by using the method in this paper

No.	Name	Type	$\lvert Var \rvert$	$\lvert Loc \rvert$	$\lvert Trans \rvert$	t_c	t_s
1	biology_1	NLC	7	1	0	8.894	20.912
2	biology_2	NLC	9	1	0	7.892	12.939
3	bouncing_ball	LC	2	1	1	8.149	11.960
4	brusselator	NLC	2	1	0	7.428	10.650
5	buckling_column	NLC	2	1	0	7.738	11.056
6	coupledVanderPol	NLC	4	1	0	8.202	11.746
7	E5	NLC	5	1	0	8.230	36.635
8	fischer_N2_flat_safe	LH	6	16	82	20.158	54.145
9	fischer_N2_flat_unsafe	LH	6	16	82	19.287	59.627
10	glycemic_control_1	NLH	5	3	4	8.319	15.385
11	glycemic_control_2	NLH	5	3	4	8.301	15.567
12	glycemic_control_poly1	NLH	4	9	18	10.528	23.938
13	glycemic_control_poly2	NLH	4	6	10	9.237	19.341
14	helicopter	LC	28	1	0	10.096	14.897
15	Hires	NLC	9	1	0	7.912	9.001
16	jet_engine	NLC	2	1	0	7.667	11.816
17	lac_operon	NLC	2	1	0	7.586	13.257
18	lorentz	NLC	3	1	0	7.739	11.253
19	lotka_volterra	NLC	2	1	0	7.740	11.025
20	circuits_n2	NLH	3	3	2	9.39	13.895
21	circuits_n4	NLH	5	3	2	8.506	14.202
22	circuits_n6	NLH	7	3	2	8.585	15.113
23	circuits_n8	NLH	9	3	2	8.624	15.386
24	circuits_n10	NLH	11	3	2	8.752	15.813
25	circuits_n12	NLH	13	3	2	9.604	19.837
26	OREGO	NLC	4	1	0	9.157	11.111
27	randgen	LH	3	3	6	9.056	15.112
28	Rober	NLC	4	1	0	8.266	16.999
29	roessler	NLC	3	1	0	9.144	12.771
30	small_circuit	NLC	5	1	0	10.265	13.660
31	spiking_neuron	NLH	2	2	2	8.703	13.559
32	spring_pendulum	NC	4	1	0	9.861	6.251
33	vanderpol	NLC	2	1	0	8.119	12.226

Column Type presents different classes of dynamics, where LC, NLC, LH, and NLH are abbreviations for linear continuous, nonlinear continuous, linear hybrid, and nonlinear hybrid, respectively. Columns $|Var|$, $|Loc|$, and $|Trans|$ show the number of variables, locations, and transitions, respectively, while t_c and t_s show, respectively, the time our tool required to translate the model, and the time to simulate the translated SLSF diagram twice

5 Conclusion

We have presented a trajectory-equivalent transformation of a hybrid automaton into a continuous-time SLSF diagram and described its implementation in a prototype software tool. For nondeterministic models, our approach adds auxiliary randomization for various sources of nondeterminism to mimic the semantics of hybrid automata. We have empirically validated our approach on a number of challenging benchmarks. To account for zero-crossing issues in the simulation engine, our translation is parameterized by an ε-relaxation; for $\varepsilon = 0$, we obtain an under-approximation of the hybrid automaton trajectories (which is precise assuming a perfect simulation engine), while for $\varepsilon > 0$ we obtain an over-approximation.

For the future, it will be interesting to further refine and extend our approach by, for example, considering the translation of *networks* of hybrid automata—directly without first composing them—into SLSF diagrams and exploring further sources of nondeterminism such as nondeterministic flows. Another direction would be to make the distribution over all possible executions uniform. A focus on rare events in the line of [17] and evaluating the SLSF diagrams using tools integrated with SLSF such as S-TaLiRo [4] or Breach [18] would also be useful.

Acknowledgements The authors thank the anonymous reviewers for their insightful comments. The material presented in this paper is based upon work supported by the Air Force Office of Scientific Research (AFOSR), in part under contract numbers FA9550-15-1-0258 and W911NF-16-1-0534, by AFRL through contract number FA8750-15-1-0105, by the National Science Foundation (NSF) under Grant Numbers CNS 1464311, EPCN 1509804, and CCF 1527398, and by the ARC Project DP140104219 "Robust AI Planning for Hybrid Systems". Any opinions, findings, and conclusions or recommendations expressed in this publication are those of the authors and do not necessarily reflect the views of AFRL, AFOSR, or NSF.

References

1. Agrawal, A., Simon, G., Karsai, G.: Semantic translation of Simulink/Stateflow models to hybrid automata using graph transformations. Electr. Notes Theor. Comput. Sci **109**, 43–56 (2004). doi:10.1016/j.entcs.2004.02.055
2. Agut, D.E.N., van Beek, D.A., Rooda, J.E.: Syntax and semantics of the compositional interchange format for hybrid systems. J. Log. Algebr. Program **82**(1), 1–52 (2013). doi:10.1016/j.jlap.2012.07.001
3. Alur, R., Kanade, A., Ramesh, S., Shashidhar, K.C.: Symbolic analysis for improving simulation coverage of Simulink/Stateflow models. In: EMSOFT, pp. 89–98. ACM (2008). doi:10.1145/1450058.1450071
4. Annpureddy, Y., Liu, C., Fainekos, G.E., Sankaranarayanan, S.: S-TaLiRo: a tool for temporal logic falsification for hybrid systems. In: TACAS, vol. 6605, pp. 254–257. Springer (2011). doi:10.1007/978-3-642-19835-9_21
5. Bak, S., Bogomolov, S., Johnson, T.T.: HYST: a source transformation and translation tool for hybrid automaton models. In: HSCC, pp. 128–133, ACM (2015). doi:10.1145/2728606.2728630
6. Bak, S., Johnson, T.T.: Periodically-scheduled controller analysis using hybrid systems reachability and continuization. In: RTSS, pp. 195–205. IEEE Computer Society (2015). doi:10.1109/RTSS.2015.26
7. Balasubramanian, D., Pasareanu, C.S., Whalen, M.W., Karsai, G., Lowry, M.R.: Polyglot: modeling and analysis for multiple statechart formalisms. In: ISSTA, pp. 45–55. ACM (2011), doi:10.1145/2001420.2001427
8. Bogomolov, S., Donzé, A., Frehse, G., Grosu, R., Johnson, T.T., Ladan, H., Podelski, A., Wehrle, M.: Guided search for hybrid systems based on coarse-grained space abstractions. STTT **18**(4), 449–467 (2016). doi:10.1007/s10009-015-0393-y
9. Bogomolov, S., Frehse, G., Greitschus, M., Grosu, R., Pasareanu, C.S., Podelski, A., Strump, T.: Assume-guarantee abstraction refinement meets hybrid systems. In: HVC. LNCS, vol. 8855, pp. 116–131. Springer (2014). doi:10.1007/978-3-319-13338-6_10
10. Bogomolov, S., Frehse, G., Grosu, R., Ladan, H., Podelski, A., Wehrle, M.: A box-based distance between regions for guiding the reachability analysis of SpaceEx. In: CAV. LNCS, vol. 7358, pp. 479–494. Springer (2012). doi:10.1007/978-3-642-31424-7_35
11. Bogomolov, S., Schilling, C., Bartocci, E., Batt, G., Kong, H., Grosu, R.: Abstraction-based parameter synthesis for multiaffine systems. In: HVC. LNCS, vol. 9434, pp. 19–35. Springer (2015). doi:10.1007/978-3-319-26287-1_2
12. Bouissou, O., Chapoutot, A.: An operational semantics for Simulink's simulation engine. In: LCTES, pp. 129–138. ACM (2012). doi:10.1145/2248418.2248437
13. Carloni, L., Di Benedetto, M.D., Pinto, A., Sangiovanni-Vincentelli, A.: Modeling techniques, programming languages, design toolsets and interchange formats for hybrid systems. Tech. Rep. (2004)
14. Carloni, L.P., Passerone, R., Pinto, A., Sangiovanni-Vincentelli, A.L.: Languages and tools for hybrid systems design. In: Foundations and Trends in Electronic Design Automation 1(1/2) (2006). doi:10.1561/1000000001
15. Chen, M., Ravn, A.P., Wang, S., Yang, M., Zhan, N.: A two-way path between formal and informal design of embedded systems. In: UTP. LNCS, vol. 10134, pp. 65–92. Springer (2016)
16. Chen, X., Ábrahám, E., Sankaranarayanan, S.: Flow*: an analyzer for non-linear hybrid systems. In: CAV. LNCS, vol. 8044, pp. 258–263. Springer (2013). doi:10.1007/978-3-642-39799-8_18
17. Clarke, E.M., Zuliani, P.: Statistical model checking for cyber-physical systems. In: ATVA. LNCS, vol. 6996, pp. 1–12. Springer (2011). doi:10.1007/978-3-642-24372-1_1
18. Donzé, A.: Breach, a toolbox for verification and parameter synthesis of hybrid systems. In: CAV. LNCS, vol. 6174, pp. 167–170. Springer (2010). doi:10.1007/978-3-642-14295-6_17
19. Duggirala, P.S., Mitra, S., Viswanathan, M.: Verification of annotated models from executions. In: EMSOFT, pp. 26:1–26:10. IEEE (2013). doi:10.1109/EMSOFT.2013.6658604
20. Fisher, M.E.: A semiclosed-loop algorithm for the control of blood glucose levels in diabetics. IEEE Trans. Biomed. Eng. **38**(1), 57–61 (1991)
21. Frehse, G., Guernic, C.L., Donzé, A., Cotton, S., Ray, R., Lebeltel, O., Ripado, R., Girard, A., Dang, T., Maler, O.: SpaceEx: Scalable verification of hybrid systems. In: Gopalakrishnan, G., Qadeer, S. (eds.) CAV. LNCS, vol. 6806, pp. 379–395. Springer (2011). doi:10.1007/978-3-642-22110-1_30
22. Hamon, G.: A denotational semantics for Stateflow. In: EMSOFT, pp. 164–172. ACM (2005). doi:10.1145/1086228.1086260
23. Hamon, G., Rushby, J.M.: An operational semantics for Stateflow. STTT **9**(5–6), 447–456 (2007). doi:10.1007/s10009-007-0049-7
24. Hybrid Automata: From verification to implementation—supplementary material. http://swt.informatik.uni-freiburg.de/tool/spaceex/ha2slsf
25. Jiang, Z., Pajic, M., Alur, R., Mangharam, R.: Closed-loop verification of medical devices with model abstraction and refinement. STTT **16**(2), 191–213 (2014). doi:10.1007/s10009-013-0289-7
26. Johansson, K.H., Egerstedt, M., Lygeros, J., Sastry, S.: On the regularization of zeno hybrid automata. Syst. Control Lett. **38**(3), 141–150 (1999)
27. Larsen, K.G., Pettersson, P., Yi, W.: UPPAAL in a nutshell. STTT **1**(1–2), 134–152 (1997). doi:10.1007/s100090050010
28. Lavalle, S.M., Kuffner, J.J., Jr.: Rapidly-exploring random trees: progress and prospects. In: Donald, B., Lynch, K., Rus, D. (eds.) Algorithmic and Computational Robotics: New Directions, pp. 293–308. A K Peters/CRC Press (2000)
29. Manamcheri, K., Mitra, S., Bak, S., Caccamo, M.: A step towards verification and synthesis from Simulink/Stateflow models. In: Proceedings of the 14th international conference on Hybrid systems: computation and control HSCC'11, pp. 317–318. ACM (2011). doi:10.1145/1967701.1967749
30. Minopoli, S., Frehse, G.: From simulation models to hybrid automata using urgency and relaxation. In: HSCC, pp. 287–296. ACM (2016). doi:10.1145/2883817.2883825
31. Minopoli, S., Frehse, G.: SL2SX translator: from Simulink to SpaceEx models. In: HSCC, pp. 93–98. ACM (2016). doi:10.1145/2883817.2883826
32. Nguyen, L.V., Johnson, T.T.: Benchmark: DC-to-DC switched-mode power converters (buck converters, boost converters, and

buck-boost converters). In: ARCH. EPiC Series in Computing, vol. 34, pp. 19–24. EasyChair (2014). http://www.easychair.org/publications/paper/Benchmark_DC-to-DC_Switched-Mode_Power_Converters_-Buck_Converters-_Boost_Converters-_and_Buck-Boost_Converters
33. Pajic, M., Jiang, Z., Lee, I., Sokolsky, O., Mangharam, R.: From verification to implementation: a model translation tool and a pacemaker case study. In: RTAS, pp. 173–184. IEEE Computer Society (2012). doi:10.1109/RTAS.2012.25
34. Pajic, M., Jiang, Z., Lee, I., Sokolsky, O., Mangharam, R.: Safety-critical medical device development using the UPP2SF model translation tool. ACM Trans. Embed. Comput. Syst. **13**(4s), 127:1–127:26 (2014). doi:10.1145/2584651
35. Pajic, M., Mangharam, R., Sokolsky, O., Arney, D., Goldman, J.M., Lee, I.: Model-driven safety analysis of closed-loop medical systems. IEEE Trans. Ind. Inform. **10**(1), 3–16 (2014). doi:10.1109/TII.2012.2226594
36. Pinto, A., Carloni, L.P., Passerone, R., Sangiovanni-Vincentelli, A.L.: Interchange format for hybrid systems: abstract semantics. In: HSCC. LNCS, vol. 3927, pp. 491–506. Springer (2006). doi:10.1007/11730637_37
37. Pinto, A., Sangiovanni-Vincentelli, A.L., Carloni, L.P., Passerone, R.: Interchange formats for hybrid systems: review and proposal. In: HSCC. LNCS, vol. 3414, pp. 526–541. Springer (2005). doi:10.1007/978-3-540-31954-2_34
38. Sampath, P., Rajeev, A.C., Ramesh, S.: Translation validation for Stateflow to C. In: DAC, pp. 23:1–23:6. ACM (2014). doi:10.1145/2593069.2593237
39. Sanfelice, R.G., Copp, D.A., Nanez, P.: A toolbox for simulation of hybrid systems in Matlab/Simulink: hybrid equations (HyEQ) toolbox. In: HSCC, pp. 101–106. ACM (2013). doi:10.1145/2461328.2461346
40. Schrammel, P., Jeannet, B.: From hybrid data-flow languages to hybrid automata: a complete translation. In: HSCC, pp. 167–176. ACM (2012). doi:10.1145/2185632.2185658
41. Severns, R.P., Bloom, G.: Modern DC-to-DC Switchmode Power Converter Circuits. Van Nostrand Reinhold Company, New York (1985)
42. Simulink Design Verifier. http://www.mathworks.com/products/sldesignverifier/
43. Tiwari, A., Shankar, N., Rushby, J.M.: Invisible formal methods for embedded control systems. Proc. IEEE **91**(1), 29–39 (2003)
44. Yan, G., Jiao, L., Li, Y., Wang, S., Zhan, N.: Approximate bisimulation and discretization of hybrid CSP. In: Fitzgerald, J., Heitmeyer, C., Gnesi, S., Philippou, A., (eds.) FM. LNCS, vol. 9995, pp. 702–720. Springer, Cham (2016) doi:10.1007/978-3-319-48989-6_43
45. Zou, L., Zhan, N., Wang, S., Fränzle, M.: Formal verification of Simulink/Stateflow diagrams. In: Finkbeiner, B., Pu, G., Zhang, L. (eds.) ATVA. LNCS, vol. 9364, pp. 464–481. Springer, Cham (2015) doi:10.1007/978-3-319-24953-7_33